Multiscale Modeling and Simulation of the Cardiac Fiber Architecture for DMRI

Lihui Wang, Yuemin Zhu*, Hongying Li, Wanyu Liu, and and Isabelle E. Magnin

***Abstract*—Cardiac fiber architecture plays an important role in the study of mechanical and electrical properties of the wall of the human heart, but still remains to be elucidated. This paper proposes to investigate, in a multiscale manner, how the arrangement patterns and morphological heterogeneity of cardiac myocytes influence the fibers orientation. To this end, different virtual cardiac fiber structures are modeled, and diffusion tensor imaging at multiple scales are simulated using the Monte Carlo method. The results show that the proposed modeling and simulation allow us to quantitatively describe the variation of the measured tissue properties (fiber orientation and fractional anisotropy) as a function of the observation scale.**

***Index Terms*—Cardiac fiber architecture, diffusion tensor imaging (DTI), multiscale simulation, myocyte modeling.**

I. Introduction

MYOCARDIAL fiber architecture plays an important role in the study of the mechanical and electrical properties of the ventricles of the human heart. It is usually mapped using diffusion tensor MRI based on the measurement of the water diffusion tensor within each voxel of magnetic resonance (MR) images [1]–[3]. The orientation of the cardiac fibers or fiber bundles in that voxel is inferred from the eigenvector of the diffusion tensor. However, diffusion tensor imaging (DTI) has a significant limitation. It is unable to resolve the intravoxel orientation heterogeneity problem such as fiber crossing and fiber kissing, due to its Gaussian diffusion assumption. In order to overcome this limitation, q-space imaging [4][1] and q-ball imaging (QBI) [5] were developed that measure the diffusion function directly from the diffusion signal by Fourier and Funk–Radon transforms without any hypothesis. However, for typical MR diffusion imaging, an image voxel is in the order of about $2\,\text{mm} \times 2\,\text{mm} \times 2\,\text{mm}$. For cardiac applications, it means that such a voxel contains thousands of cardiac myocytes and other extracellular tissues. In this condition, it is difficult to exactly know the relationship between the measured macroscopic fiber orientation and the microscopic cardiac myocyte arrangement. In order to get rid of the limitations of these imaging techniques, a few modeling and simulation methods have been reported in the literature. In [6], the Brownian motion of molecules was simulated using the Monte Carlo method in a restricted space to obtain the diffusion signal. In [7], the diffusion anisotropy was simulated with a fiber phantom. The authors of [8] compared the experimental diffusion signal and the simulated signal for a cylinder fiber. However, these works were realized only for simple diffusion environments and on 1-D diffusion signals. Moreover, the reported works do not deal with the calculation of diffusion-weighted images in the restricted environment.

In this paper, we propose to model realistic diffusion environments and calculate the subsequent 3-D diffusion images. More precisely, virtual cardiac fiber structures (VCFSs) are modeled, and the diffusion behavior of water molecules is simulated in this VCFS using the Monte Carlo method. Furthermore, the virtual diffusion MR images and the orientation of fibers at different scales are calculated based on DTI. Finally, the influence of the heterogeneity of the cardiac myocyte structure on the simulated tensor eigenvectors and fractional anisotropy (FA) is analyzed by changing the size and the arrangement patterns of the myocytes.

II. Theory

A. VCFS Model

According to histological parameters, the myocytes are modeled by a series of cylinders whose diameters range from 5 to 25 μm and length from 50 to 100 μm [9]. Since the spatial resolution of conventional MR images is about 2 mm, and the myocyte density is about 0.2×10^8 cells/cm^3 [10], thus, in one voxel of an MR image there are about 50 000 myocytes. These myocytes have in general different orientations whose variance depends on the myocyte location. This means that, at the apex, the divergence of the myocyte orientations can be up to 90°, whereas in the middle wall it is less than 10° [9]. Meanwhile, the arrangement pattern of myocytes is always a debatable issue. In the present study, both cardiac sheet and cardiac random patterns are simulated. All the aforementioned elements (shapes, arrangement pattern, and orientation divergence) constitute the cardiac myocyte structure heterogeneity in one voxel. In order

Manuscript received April 2, 2011; revised June 10, 2011; accepted August 9, 2011. Date of publication August 30, 2011; date of current version December 21, 2011. This work was supported in part by the National Natural Science Foundation of China under Grant 60777004, in part by the International S&T Cooperation Project of China under Grant 2007DFB30320, in part by the French National Research Agency 2009 under Grant ANR-09-BLAN-0372-01, and in part by the Region Rhone-Alpes of France under the Project CIBLE 2010. *Asterisk indicates corresponding author.*

L. Wang and W. Liu are with the Harbin Institute of Technology, Harbin 150001, China, and also with CREATIS, CNRS UMR5220, Inserm U1044, INSA Lyon, University of Lyon1,University of Lyon, Villeurbanne 69100, France (e-mail: lihui.wang@creatis.insa-lyon.fr; wanyu.liu@hit.edu.cn).

*Y. Zhu is with CREATIS, CNRS UMR5220, Inserm U1044, INSA Lyon, University of Lyon1, University of Lyon, Villeurbanne 69100, France (e-mail: yuemin.zhu@creatis.insa-lyon.fr).

H. Li and I. E. Magnin are with CREATIS, CNRS UMR5220, Inserm U1044, INSA Lyon, University of Lyon1, University of Lyon, Villeurbanne 69100, France (e-mail: hongying.li@creatis.insa-lyon.fr; isabelle.magnin@creatis.insa-lyon.fr).

Color versions of one or more of the figures in this paper are available online at http://ieeexplore.ieee.org.

Digital Object Identifier 10.1109/TBME.2011.2166265

to analyze their respective influence, the VCFS model is divided into several groups.

1) Myocytes bear the same orientation but with various sizes.
2) Myocytes are arranged in a cardiac tissue sheet manner.
3) Myocytes are arranged randomly.

B. Diffusion MRI (DMRI) Simulation Basis

The diffusion process can be seen as a sequence of tiny random walks of water molecules. If the walk of molecules obeys the stochastic properties of a Brownian particle, the random 3-D walking displacement Δ of a molecule i during time interval δt between two random walks is then given by [11]

$$\Delta \vec{r}_i = \sqrt{2mD_0\delta t} \tag{1}$$

where D_0 is the diffusion coefficient of water molecules, m is the diffusion dimension, and δt is the diffusion time for each walk step.

According to the basic theory of DMRI [11], the phase shift induced by this displacement is

$$\Delta\phi_i = 2\pi \vec{q} \cdot \Delta \vec{r}_i \tag{2}$$

where $\vec{q}$ is related to the diffusion gradient $\vec{G}(t)$, $q = \frac{\gamma}{2\pi} \int \vec{G}(t)dt$ with γ designating the gyromagnetic ratio.

Thus, the diffusion signal can be numerically approximated by

$$E(\Delta\phi) = \frac{1}{n}\sum_{i=1}^{n} \cos(\Delta\phi_i), \quad \Delta\phi_i \in \text{support of } P(\Delta\phi) \tag{3}$$

where n designates the number of molecules involved and i is the index of the molecules. The phase $\Delta\phi_i$ should conform to the distribution $P(\Delta\phi)$. By combining (2) and (3), the diffusion signal can be further written as

$$E(\Delta\phi) = \frac{1}{n}\sum_{i=1}^{n} \cos(2\pi \vec{q} \cdot \Delta \vec{r}_i), \ \Delta \vec{r}_i \in \text{support of } P(\Delta \vec{r}). \tag{4}$$

If the diffusion gradient is a constant, according to (2), the distribution $P(\Delta)$ will be the same as $P(\Delta\phi)$. In this paper, this distribution is simulated by a Monte Carlo method. For the random walking direction, it conforms to the uniform distribution from 0 to 2π. The distance s for each walk step is a constant, and determined by the diffusion coefficient expressed as in (1). Designating the total diffusion time as Δ, then the number of random walk steps k for one molecule is

$$k = \frac{\Delta}{\delta t}. \tag{5}$$

If the displacement for the ith molecule induced by the j^{th} walk step is $\Delta \vec{r}_{ij}$, the corresponding phase shift is

$$\phi_{ij} = 2\pi \vec{q} \cdot \Delta \vec{r}_{ij}. \tag{6}$$

At the end of the diffusion, the total phase shift for the ith molecule is

$$\phi_i = \sum_{j=1}^{k} \phi_{ij} = \sum_{j=1}^{k} 2\pi \vec{q} \cdot \Delta \vec{r}_{ij}. \tag{7}$$

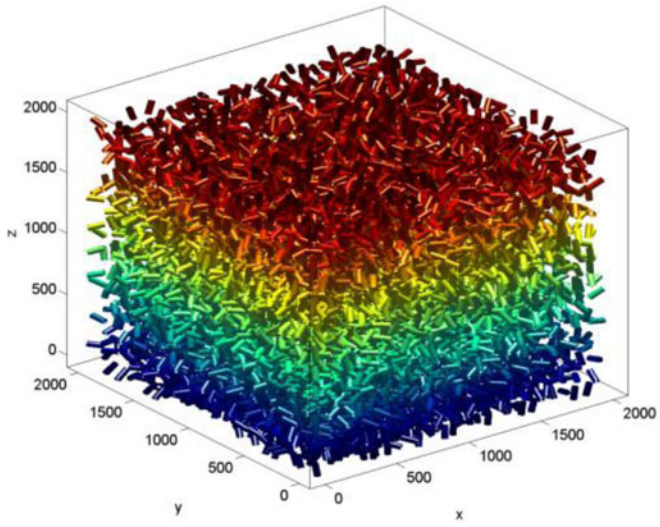

Fig. 1. Simulation of a 2 mm × 2 mm × 2 mm voxel containing 20 × 20 × 20 myocytes having the same size but arranged randomly (uniform distribution).

According to (4), we then obtain the diffusion signal

$$E(\phi) = \frac{1}{n}\sum_{i=1}^{n} \cos(\phi_i) = \frac{1}{n}\sum_{i=1}^{n} \cos\left(\sum_{j=1}^{k} 2\pi \vec{q} \cdot \Delta \vec{r}_{ij}\right). \tag{8}$$

Due to the fact that water molecules diffuse in a restricted VCFS environment, the interaction between the molecules and the membrane of the myocyte should be considered in the simulation. In this paper, such interaction is modeled by elastic collision and reflection, which means that, after the collision with the membrane, the molecule does not lose energy and will be reflected by the membrane in an arbitrary direction.

III. Experiments and Results

A. VCFS Models

Following the histological knowledge, the myocytes in this paper are modeled by cylinders, which diameter ranges from 5 to 25 μm and length varies from 50 to 100 μm. The orientation of the myocytes is determined by both the elevation and azimuth angles. The elevation angle is randomly selected between 0 and π, and the azimuth from 0 to 2π. In Fig. 1, the VCFS model is illustrated formed of a volume of 20 × 20 × 20, where the myocytes have the same size (diameter 20 μm, and length 100 μm), and their arrangement pattern is random and independent of their orientation. In Fig. 2, the myocytes are arranged according to an orientation similarity, which allows simulating the sheet structure of myocytes. In order to analyze the influence of size variation on the fiber orientation measurement, the VCFS model with different myocyte sizes and ratios of length to diameter but the same arrangement pattern as in Fig. 1 is considered, as illustrated in Fig. 3. The myocytes in these three models are taken as groundtruths in what follows.

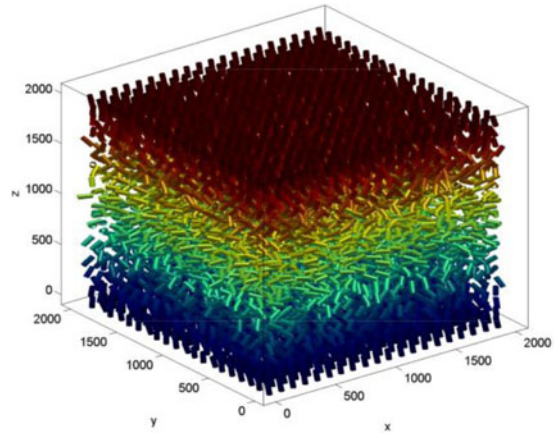

Fig. 2. Simulation of a 2 mm × 2 mm × 2 mm voxel containing 20 × 20 × 20 myocytes having the same size and arranged regularly.

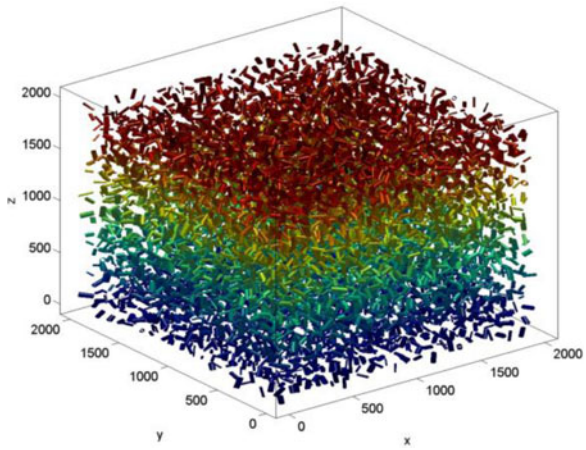

Fig. 3. Simulation of a 2 mm × 2 mm × 2 mm voxel containing 20 × 20 × 20 myocytes having random sizes and arranged randomly.

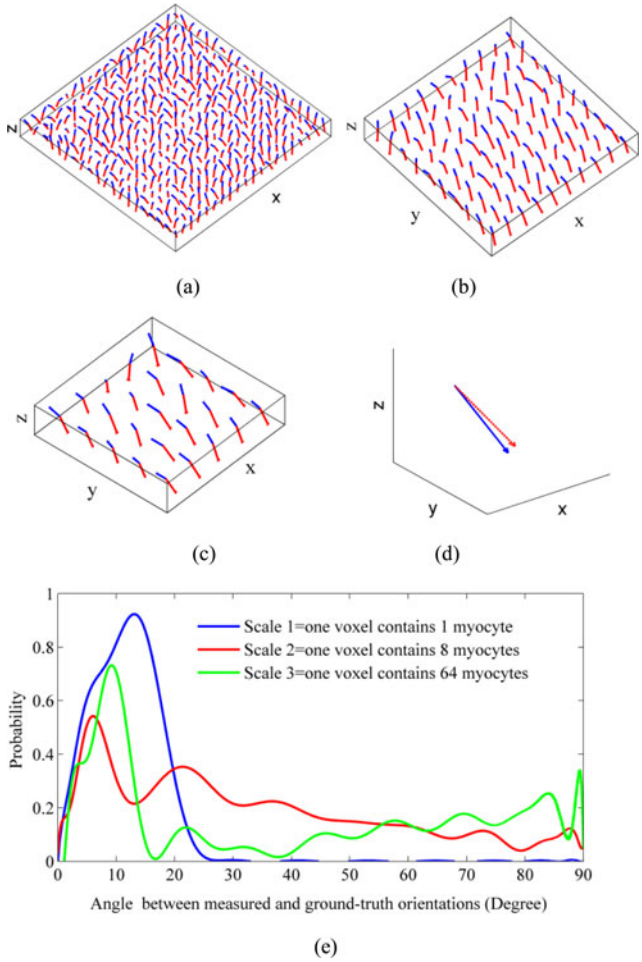

Fig. 4. Results of measurement of fiber orientations and probability distribution of fiber orientation deviations as a function of voxel size (observation scales). Measured (red) and groundtruth (blue) orientations. (a) At scale 1 = one voxel contains 1 myocyte. (b) At scale 2 = one voxel contains 8 myocytes. (c) At scale 3 = one voxel contains 64 myocytes. (d) At scale of 20 × 20 × 20 = 8000 myocytes. (e) Comparison of probability distributions of fiber orientation deviations between measured and groundtruth at different scales.

B. Simulation of Fiber Orientations at Different Scales

As stated in the previous section, DMRI data can be simulated by applying diffusion gradients along different directions. In this paper, the number of diffusion directions defined by icosahedrons is 162, and the diffusion gradient magnitude is 3 T/μm. The number of water molecules in each myocyte is 5000, and the diffusion time is 60 ms.

In order to investigate the influence of observation scales on the measurement of diffusion orientations, the diffusion tensor images corresponding to one slice (axial slice 3) in the model of cardiac fiber sheet structure (see Fig. 2) are calculated at different scales. According to (8), for different gradient directions, we calculate different diffusion signals from which the diffusion tensors are derived [3]. The primary eigenvector of the tensor is taken as the measured diffusion orientation, as shown by the red color vectors in Fig. 4. At the microscale, the orientation of the cylinders in the VCFS models is taken as the reference or groundtruth orientation. At the meso- and macroscales, the groundtruth orientation is based on the previous microscale reference, and is given by the average orientation of the cylinders inside the voxel corresponding to the given scale. In Fig. 4, the groundtruth orientation is indicated by blue color vectors.

From the probability distribution curves in Fig. 4(e), it can be seen that, from microscopic to macroscopic scales, the measured diffusion orientation deviates more and more from the groundtruth. At microscale (scale 1), the distribution of angles between the measured and groundtruth orientations is located mainly in the interval [0°, 25°]. However, at mesoscale (scale 2) and macroscale (scale 3), the angle distribution spreads almost over the entire interval [0°, 90°], which implies that, with conventional DMRI, the measured fiber orientations might greatly deviate from the actual ones.

Now, in order to analyze the influence of arrangement patterns and size variation on diffusion measurement for the same scale (one voxel contains 20 × 20 × 20 = 8000 myocytes), but with the three different models (see Figs. 1–3), myocyte orientations and FA values are measured (see Fig. 5). We remark that different myocyte sizes and arrangement patterns lead to different measured fiber orientations, and that it is the myocyte

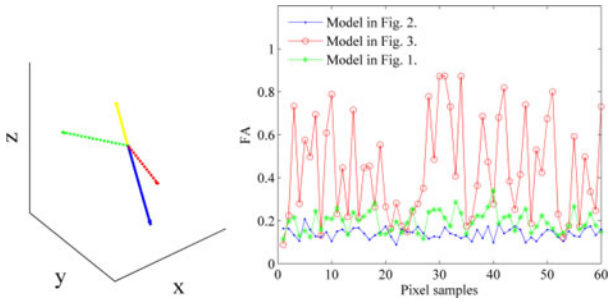

Fig. 5. Measured fiber orientations and FA values for the three models: model 1 (see Fig. 1), model 2 (see Fig. 2), and model 3 (see Fig. 3).

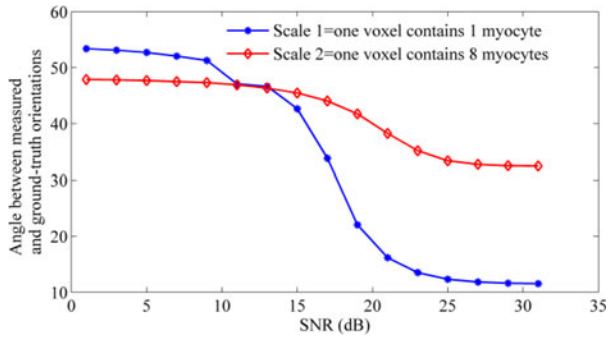

Fig. 6. Noise influence on the choice of optimal voxel sizes.

size (ratio of length to diameter) that causes the most important changes both in FA and in the variation of the latter.

The aforementioned measurement results with the same scale or different scales demonstrate that the variation of arrangement patterns and myocyte sizes influences the macroscopically measured fiber orientation and FA. This means that we can generate various simulation configurations with different microscopic arrangements and myocyte sizes to understand the relationship between microscopy and macroscopy, and predict microstructure information from macroscopic measurements.

C. Noise Influence on the Choice of Optimal Voxel Sizes

In noise-free cases, as described in Section III-B, the smaller the voxel size, the more accurate the orientation measurement is. In noisy cases, there is, however, a compromise between voxel size and signal-to-noise ratio (SNR) of diffusion signals. To investigate the choice of optimal voxel sizes, we simulated different noise levels at two different scales (scales 1 and 2). In this paper, we considered only the displacement noise with Gaussian distribution (mean value is 0), and the SNR defined by

$$\mathrm{SNR} = 20 \times \log\left(\frac{\max(\text{molecule displacements})}{\sigma}\right) \quad (9)$$

with σ designating the variance of the noise.

Fig. 6 represents the variation of angles between the measured and groundtruth fiber orientation as a function of SNRs for two different scales. We observe that the orientation deviation is much more sensitive to noise at smaller voxel size (scale 1) than at bigger voxel size (scale 2). Meanwhile, when the SNR is lower than 15 dB, the simulation at larger scale gives better results than at smaller scale, which means that, for lower SNRs, the optimal voxel size should be bigger.

IV. Conclusion

We have proposed three different VCFS models, and simulated their corresponding diffusion tensor images at different scales using the Monte Carlo method. The results show that, at microscopic scale, the measured fiber orientations are in agreement with the groundtruth, while, at macroscopic scales, the measured fiber orientation can significantly deviate from groundtruth. From microscopy to macroscopy, the larger the observation scale, the more the obtained results may deviate from groundtruth. Moreover, the results show that FA changes dramatically with the variation of myocyte sizes but smoothly with that of arrangement patterns. These results suggest that, using the proposed multiscale modeling and simulation, the relationship between microscopic structure heterogeneity and macroscopic measurements will allow us to predict microscopic tissue structure and explain macroscopic behaviors, not just resolve the intravoxel orientation heterogeneity problem (such as fiber crossing and fiber kissing) as done, for example, by QBI. Finally, the presence of noise raises the problem of choosing optimal voxel sizes; when SNR is lower, bigger voxel sizes will yield better results than smaller ones.

References

[1] P. B. Kingsley, "Introduction to diffusion tensor imaging mathematics: Part I. Tensors, rotations, and eigenvectors," *Concepts Magn. Reson. Part A*, vol. 28, pp. 101–122, 2006.

[2] P. B. Kingsley, "Introduction to diffusion tensor imaging mathematics: Part II. Anisotropy, diffusion-weighting factors, and gradient encoding schemes," *Concepts Magn. Reson. Part A*, vol. 28, pp. 123–154, 2006.

[3] P. B. Kingsley, "Introduction to diffusion tensor imaging mathematics: Part III. Tensor calculation, noise, simulations, and optimization," *Concepts Magn. Reson. Part A*, vol. 28, pp. 155–179, 2006.

[4] E. Özarslan, C. G. Koay, and P. J. Basser, "Remarks on q-space MR propagator in partially restricted, axially-symmetric, and isotropic environments," *Magn. Reson. Imag.*, vol. 27, pp. 834–844, 2009.

[5] D. S. Tuch, "Q-ball imaging," *Magn. Reson. Med.*, vol. 52, pp. 1358–1372, 2004.

[6] A. Duh, A. Mohori, and J. Stepinik, "Computer simulation of the spin-echo spatial distribution in the case of restricted self-diffusion," *J. Magn. Reson.*., vol. 148, pp. 257–266, 2001.

[7] E. Fieremans, Y. De Deene, S. Delputte, M. S. Özdemir, Y. D'Asseler, J. Vlassenbroeck, K. Deblaere, E. Achten, and I. Lemahieu, "Simulation and experimental verification of the diffusion in an anisotropic fiber phantom," *J. Magn. Reson.*, vol. 190, pp. 189–199, 2008.

[8] L. Avram, E. Özarslan, Y. Assaf, A. Bar-Shir, Y. Cohen, and P. J. Basser, "Three-dimensional water diffusion in impermeable cylindrical tubes: Theory versus experiments," *NMR Biomed*, vol. 2, pp. 888–898, 2008.

[9] N. J. Severs, "The cardiac muscle cell," *Bioessays*, vol. 22, pp. 188–199, 2000.

[10] M. Radisic and G. V. Novakovic, "Cardiac tissue engineering," *J. Serb. Chem. Soc.*, vol. 70, pp. 541–556, 2005.

[11] J. B. Heidi and E. J. B. Timothy, "*Diffusion MRI,*" 1st ed. New York: Elsevier, 2009, pp. 8–10.